Friedrich Schiller Universität Jena
PAF

Dissertation

High-Fluence Ion Beam Irradiation of Semiconductor Nanowires

Andreas Johannes

März 2015

Abstract

Hier alles Bla

Contents

1 Introduction

We are living in an era dominated by the information technology (IT). There is virtually no part of life not influenced by the continuing advances in the digital world and semiconductors, especially silicon, are at the base of each and every logic unit dealing in 'ones' and 'zeros'. Some technological advances were triggered by fundamentally new effects such as the giant magneto-resistance (GMR) discovered in 1988. This is the basis for the standard hard-drives (HDD) as we know them. The HDDs however are already being replaced with so called solid state drives (SSD) which are based on flash memory. They owe their viability (cost, speed and storage density) almost entirely to the ability to produce a floating gate for a transistor on a scale down to tens of nanometers per single *bit* and while producing billions of $bits/cm^2$. There is thus a competition between shear 'brute force' miniaturization and the development of fundamentally new operation principles. This competition can be found in the "International Technology Roadmap for Semiconductors" which aims to guide the scaling of devices to follow "Moore's Law" of improved performance and the white paper "Towards a "More-than-Moor" roadmap" which examines opportunities to include non-digital functionalities where performance don't necessarily have to scale with size (both available at the ITRS website [rm15]). The competition between classical and quantum computing will be a particularly interesting example of this to follow in the near future.

As a side effect of miniaturization being a major factor in the improvement of all IT-hardware-technology, nanotechnology became somewhat of a buzzword. Fueled by this upwind for everything 'nano', a peculiar class of materials gained some academic interest: nanowires [XYS$^+$03, LW07]. 'Nanowire' is a term used for many morphologies, but it seems a reasonable name for structures with a cross-section that is between 1×1 and $1000\times1000\,nm^2$, which are significantly longer than they are wide. One of the general aspects of this shape and also of nanostructured materials in general, is that the surface properties play a dominating role. This is simply caused by the fact, that there is a lot of surface per volume of material. The surface of non-fractal body scales with the characteristic length r as r^2 while the volume follows r^3, therefore, the surface to volume ratio, proportional to $1/r$, gets very large for small structure sizes. Investigating nanowires as catalysts or sensing devices tries to take advantage of this large active surface area. The wire shape in particular has an inherent advantage here over three dimensionally constrained particles (nanoclusters, quantum dots etc.), in that it is easier to define contacts to and drive a current through a wire than through a point. The idea to combine this specific advantage of nanowires with new properties obtained by the stronger three dimensional confinement of quantum dots is the main idea behind the 'Deutsche Forschungsgemeinschaft' (DFG) project "wiring quantum dots" which funded this work.

Having somewhat motivated the use of semiconductor nanowires and before going into further detail on this specific project, first the "ion beam irradiation" part of the tile also needs an introduction. Although Si is the material of choice for microchips (hence "Silicon Valley"), as it is, pure silicon is a rather uninteresting material. The defining property of semiconductors is the ability to dramatically change their electronic properties by adding impurities [SN06]. As ion beam irradiation can be used to 'mix' (i.e. dope) virtually any target material with a precisely controlled number of atoms of practically any element, it was and is a key part in the processing and development of semiconductor technologies. A specific example in which the combination of nanostructures and ion beams is advantageous is the ion irradiation of diamond to create nitrogen-vacancy clusters. These are interesting as promising components in a future quantum information device [BHK+10]. The precise control ion irradiation gives makes it possible to implant a well defined number of ions with reasonable spacial accuracy. This control is extravagantly demonstrated by the possibility of single ion irradiation [MVB+06, Ohd08].

In general, ion beam doping has the advantage over doping during the synthesis of nanostructures, in that it is not inherently limited by the chemical potentials and dynamics which typically have to be carefully controlled for the synthesis of nanostructures. It is a non-equilibrium physical process by which different elements can forcefully be introduced into a target matrix with much higher energies than those involved in chemical bonding. The extent of disorder created in the target during this bombardment, whether the intermixing is thermodynamically stable, and whether a desired (crystal) order can be reestablished by thermal annealing is in the focus of ion-beam physics. A good background on this can be gained from dedicated literature [ZLB85, Nas08, Sch12, Eck91].

Following these considerations, a further concurrence of nanotechnology and ion-irradiation is found in the search for a diluted magnetic semiconductor by implanting Mn in $GaAs$ nanowires. As $GaAs$ nanowires typically grow above $450°C$ but $MnAs$ segregates from $Ga_{(1-x)}Mn_xAs$ at $350°C$ [DO06, SSK+11], there is no practicable way to dope $GaAs$ with high concentrations of Mn during nanowire growth. The key insight was to do the irradiation at elevated temperatures, hot enought to minimize disorder, but cold enough to prevent segregation [BMB+11, PKB+12, Bor12, KPJ+13, PKJ+14]. In the before mentioned "wiring quantum dots" project such segregation was actually utilized to combine nanowires with nanoclusters. When Si nanowires are irradiated with high fluences of Ga and As and subsequently annealed with a flash-lamp, separated $GaAs$ slices forme within the Si nanowires [PGL+14, Gla15]. The supersaturation of Si with Ga and As by ion implantation can thus be utilized to create $GaAs - Si$ nanowire hetero-structures from a Si nanowire template in a relatively straight-forward manner.

A further example of the intersection of nanotechnology and ion beams is found in the ubiquitous focused-ion-beam (FIB) systems. The production and development of many of the novel applications of nanostructures on the horizon often requires the precise ion-beam milling that FIBs provide with a resolution of few nanometers. In all the examples given so far, and virtually per definition in the last one, typical structure sizes irradiated are in the order of magnitude of the irradiating ions. This warrants general investigations of the nanostructure - ion beam interaction [Bor12, GHB+13, NSUM14, JHMR15]. In the effort to understand principles and fundamental interactions on the nanometer length scales, nanowires are a very good model system to investigate as their geometry is fully characterized by their height and radius. Spheres, which would have a degree of freedom less, are unfortunately more difficult to handle, as the unavoidable proximity of a substrate may influence their behavior

[Mö14, JHMR15]. Results obtained with nanowires are principally transferable to any nanostructure, however, this cannot of course be done in any general way explicitly, as the possible shapes are uncountable. This dissertation add to the growing field of nanostructure - ion beam interaction the discussion of three effects which are especially important in high fluence irradiation and dedicates a seperate chapter to each.

Chapter 3 - Sputtering of Nanowires
: In the dissertation of Dr. C. Borschel [Bor12] the program *iradina* [BR11] was developed and used to simulate the ion irradiation of nanostructures. It predicts an enhanced, diameter dependent sputter yield in nanoparticles. This chapter discussed the simulation and compares its predictions with experimentally obtained diameter dependent sputtering in nanowires. Some first results on the sputtering in the Mn irradiation of $GaAs$ were obtained and published elsewhere [JNP$^+$14]. The results presented here are on Ar irradiated Si nanowires. They were obtained in close cooperation with Stefan Noack in his M.Sc. and also published *publish* .

Chapter 4 - High Doping Concentrations in Nanowires
: The concentration of dopants does not follow a linear increase with the fluence of ions implanted for high fluences. It has already been observed in the early days of investigations into ion implantation that sputtering of the target will dynamically change its composition during the ion irradiation in addition to the intended change by incorporation of the ions within the target material [MEB88, Mö14]. This effect is enhanced in nanostructures, first since the sputtering is enhanced when compared to bulk samples as shown in the previous chapter, but also since there is simply less material in the structure. Hence, the effect of removing material by sputtering becomes significant at lower fluencies. The presented results are acquired by nano-XRF performed on 175 keV Mn$^+$ ion irradiated ZnO nanowires [JNP$^+$14]. They are discussed in comparison to a pseudo-dynamic simulation performed using results from *iradina*.

Chapter 5 - Plastic Flow in Silicon Nanowires
: In the high ion fluence irradiated Si nanowires a peculiar tendency

of the nanowires to become shorter was observed. This chapter presents a dedicated investigation into this plastic deformation of Si under ion irradiation which has been previously seen only in high energy ($\geq MeV$) ion irradiations [Vol91, TR95, HKW04, HKW05].

2 Methods

Ausgiebige Verwendung von *iradina* [BR11]

3 Sputtering of Nanostructures

When an energetic ion hits a solid target the ensuing collision cascade will displace some of the target atoms from their original positions. The energy lost by the ion in these collisions is called “nuclear” energy loss. A displaced target atom can either become an interstitial, if it stays within the target volume, or be sputtered if it has sufficient energy to leave the solid. The energy required to leave the target is the surface-binding-energy.

4 High Doping Concentrations in Nanostructures

5 Plastic Flow in Nanostructured Silicon

It was mentioned before that within the "wiring quantum dots" project Si nanowires where irradiated with As^+ and In^+ and/or Ga^+ so that in a subsequent annealing step $Si-GaAs$ or $Si-InGaAs$ hetero-structures could be formed. Markus Glaser the Ph.D. student responsible for this part of the project had developed a good habit of making SEM images of the same individual wires after each process step. We thus noticed, that the Si nanowires shrank quite dramatically during the irradiation with $\approx 100\,keV$ In^+, Ga^+ and As^+ at room temperature. Two examples of this can be seen in figure *Figure* ??. A quick look into literature revealed that this behavior has not been observed at such low ion energies. A thorough investigation might be worthwhile. Similar Si nanowire arrays as the ones used for the sputtering experiment were thus systematically irradiated with Ar^+ to avoid any chemical effects, making SEM images after each irradiated fluence to observe and quantify the deformation.

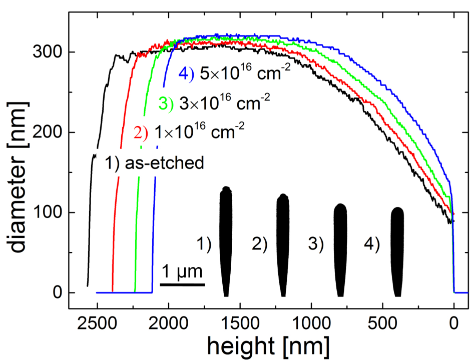

Figure 5.1: Graphs of the diameter over height of a single Si nanowire irradiated with increasing fluences of $100\,keV\,Ar^+$ ions. The black insets show the profiles of the nanowire after the respective fluences extracted from SEM images. In both illustrations the shrinking and widening of the wire is clearly visible.

Using the algorithm described in the sputter yield chapter, the profiles for the irradiated nanowires could be extracted. In figure 5.1 the black, red, green and blue lines indicate the height dependent diameter of a single wire before and after irradiation with $100\,keV Ar^+$ up to fluences of 1, 3 and $5 \times 10^{16}\,cm^{-2}$ respectively. In this graph, as well as in the inset black profiles, the reduction of the height by $\approx 500\,nm$ and an increase of the diameter, especially at the base, can be clearly seen.

In the collision cascade following an energetic ion impinging a solid will preferentially knock-on atoms along the propagation direction of the impinging ion. This causes an inhomogeneous distribution of interstitials and vacancies and effectively mass is transported 'downstream' along the ion beam. In an amorphous material it is not clear what constitutes an 'interstitial' or a 'vacancy', but a local excess of vacancies can be understood as a locally decreased density, while an interstitial excess corresponds to an increased density. A local density gradient is not stable, since the density of amorphous Si before and after irradiation is not significantly different [PMB04]. Therefore the density gradient introduces stress in the material which can relax by plastic deformation, possibly enabled by a decreased viscosity due to further ion irradiation.

As it was shown in the previous chapters that the BCA simulation software can accurately reproduce the collision cascades, let us see whether the deformation observed in the experiment can be accounted for with this knock-on mass transport. Figure 5.2a) shows the simulation volume implemented in *iradina* with $2 \times 2 \times 2\,nm^3$ voxels as a $600\,nm$ long Si cylinder with a diameter of $200\,nm$. The $100\,keV$ Ar^+ ions impinge at an angle of 45° to the z-axis. They striking the cylinder distributed uniformly along the y-direction at height $z = 0$. Figure 5.2d) shows the resulting distribution of interstitials on the cross-sectional slice through the middle of the nanowire along the xz plane. This can be seen as an approximation for the distribution of the nuclear energy loss and shows the mean extent of collision cascade. Figure 5.2e)shows the same cross-section after subtracting the distribution of the vacancies. The excess of vacancies along the impinging plane (blue line in the cross section) enveloped by two red planes of excess interstitials shows that there is a high probability for the ions to hit a target atom with a large impact parameter. This changes the ions path only little and displaces the target atom in an direction perpendicular to the ion beam. Superimposing many collisions along the y direction leads to the formation of two interstitial rich and one vacancy rich planes. The xy-plane in 5.2b) shows the sum over the height z of the difference between interstitials and vacancies plotted to the same color scale. The illustration is dominated by vacancies at the surface of the cylinder which are left behind by sputtered atoms.

The height distribution (summing over the radial xy plane) of the interstitials, vacancies and leaving atoms is shown in 5.2c). As expected, the majority of sputtered atoms originate near the impact height. The lines showing the interstitials and vacancies overlap in this illustration. Subtracting the vacancies from the sum of interstitials and leaving atoms and their the distribution along the height is plotted in f). As a displaced atom which is either sputtered or becomes an interstitial always leaves behind a vacancy, the sum over all heights of this plot is zero. The strong oscillation around $z = 0$ is caused by the previously discussed perpendicular displacement of target atoms for large impact parameters. This oscillation is very sensitive to the voxel-size as interstitial and vacancy rich regions are superimposed for larger voxels. The excess of vacancies near the impact point ($\leq 70\,nm$) and of interstitials further down along the ion's path ($\approx 100\,nm$) is not sensitive to the voxel size. It can be used to quantify the knock-on mass transport by multiplying the plotted values by their height and integrating over all heights. At this point the influence of the short range oscillation immediately around the impact point disappears as here z is small. The value obtained from this analysis is $78 \pm 1\,atoms \cdot nm/ion$.

BCA software typically checks at each collision whether the target atom acquires more energy than the “displacement energy” which is a material specific parameter. If the displaced atoms has less than the displacement energy, it is assumed, that it remains bound in its place, and that the energy is converted into lattice vibrations (= heat).

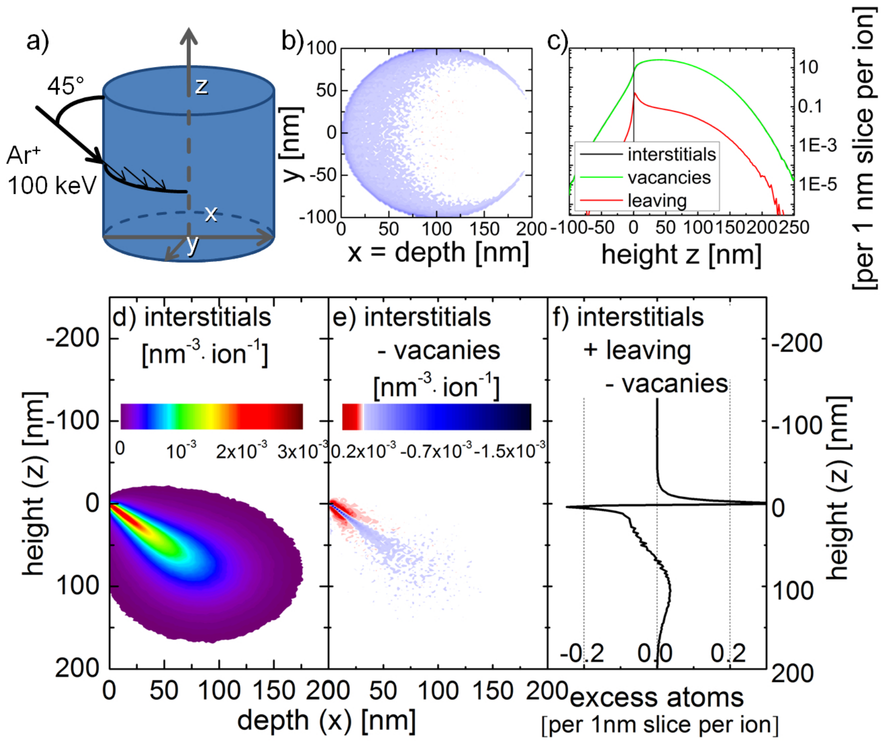

Figure 5.2: a) Illustration of the simulated irradiation geometry. All Ar^+ ions of 100 keV energy hit the nanowire volume at the same height and at an angle of 45° with respect to the wire axis z. The created interstitials in the radial cross-section through the middle of the simulated nanowire is shown in d). This distribution is effectively an illustration of the nuclear energy loss. In e) the vacancies are subtracted from the interstitials for the same cross-section. Summing this difference over all heights gives the radial distribution shown in b). The clear dominance of vacancies near the surface is caused by sputtering. The axial profile of the interstitials, vacancies and leaving (sputtered) atoms plotted in c) over the height relative to the impact plane shows, that most atoms are sputtered at the impact height. Note that the plots of vacancies and interstitials overlap. The vacancies subtracted from the sum of interstitials and sputtered atoms plotted over the height in f) shows mass transport along the ions path. Apart from the strong oscillation at the impact height, there is a deficiency of atoms close to the impact height ($\leq 70\,nm$) and an excess centered around 100 nm down from the impact height.

test

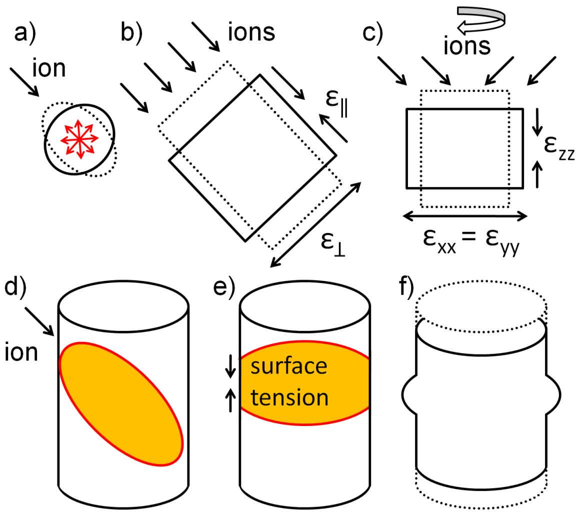

Figure 5.3: a) - c) Illustration of an deformation model analogous to ion hammering. a) The collision cascade from a single impinging ion heats an approximately ellipsoidal volume of the target material. The internal pressure will lead to an expansion towards a more spherical shape, which is retained upon cooling. b) The net effect of many ions is thus a contraction parallel to and an expansion perpendicular to the ion beam. For no change in density $\epsilon_{\parallel} = -2\epsilon_{\perp}$ has to hold. c) Under rotational symmetry this deformation translates to a contraction in the rotational axis z and an expansion in the perpendicular $x-y$ plane with $\epsilon_{zz} = -2\epsilon_{xx} = -\epsilon_{\perp}$. In d) - f) the alternative, surface tension driven deformation is illustrated. The collision-heated volume of target material shown in d). A significant slice of the wire shown in e) thus has a reduced viscosity. The surface energy is reduced by an increase in the local diameter of the wire, leading to a shortened and thickened wire segment shown in f).

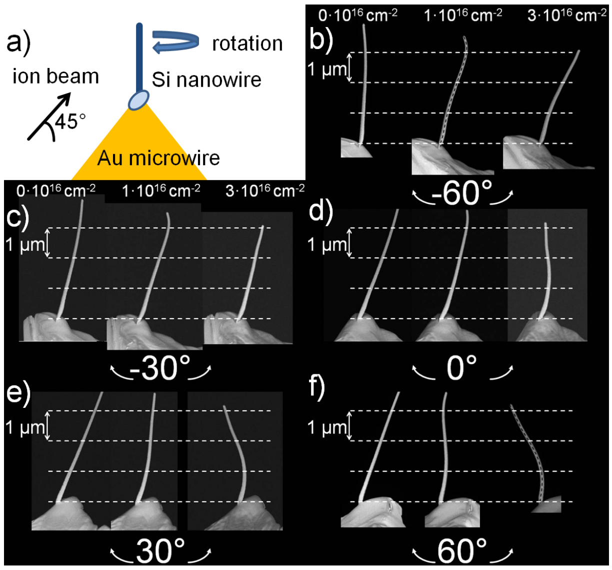

Figure 5.4: a) Illustration of the nanowire-on-microwire irradiation setup. b) - f) SEM images of the same nanowire as-mounted (left SEM images), after irradiation with $1 \times 10^{16}\, cm^{-2}$ (center images), and $3 \times 10^{16}\, cm^{-2}$ (right images) $100\, keV\, Ar^{+}$ ions. The SEM images where taken with the nanowire rotated by the indicated angle from an angle perpendicular to the angle of rotation. The length of the nanowire after irradiation is determined in b) and f) along the dashed lines.

6 Summary and Outlook

test

Bibliography

[BHK+10] Thomas M. Babinec, Birgit J. M. Hausmann, Mughees Khan, Yinan Zhang, Jeronimo R. Maze, Philip R. Hemmer, and Marko Lončar. A diamond nanowire single-photon source. *Nature Nanotechnology*, 5(3):195–199, March 2010.

[BMB+11] Christian Borschel, Maria E. Messing, Magnus T. Borgstrom, Waldomiro Paschoal, Jesper Wallentin, Sandeep Kumar, Kilian Mergenthaler, Knut Deppert, Carlo M. Canali, Hakan Pettersson, Lars Samuelson, and Carsten Ronning. A New Route toward Semiconductor Nanospintronics: Highly Mn-Doped GaAs Nanowires Realized by Ion-Implantation under Dynamic Annealing Conditions. *Nano Letters*, 11(9):3935–3940, September 2011. WOS:000294790200073.

[Bor12] Christian Borschel. *Ion-Solid Interaction in Semiconductor Nanowires*. PhD thesis, University Jena, Jena, 2012.

[BR11] C. Borschel and C. Ronning. Ion beam irradiation of nanostructures – A 3d Monte Carlo simulation code. *Nuclear Instruments and Methods in Physics Research Section B: Beam Interactions with Materials and Atoms*, 269(19):2133–2138, October 2011.

[DO06] Tomasz Dietl and Hideo Ohno. Engineering magnetism in semiconductors. *Materials Today*, 9(11):18–26, November 2006.

[Eck91] Wolfgang Eckstein. *Computer Simulation of Ion-Solid Interactions*. Springer Berlin Heidelberg, Berlin, Heidelberg, 1991.

[GHB+13] G. Greaves, J. A. Hinks, P. Busby, N. J. Mellors, A. Ilinov, A. Kuronen, K. Nordlund, and S. E. Donnelly. Enhanced Sputtering Yields from Single-Ion Impacts on Gold Nanorods. *Physical Review Letters*, 111(6):065504, August 2013. 00004.

[Gla15] Markus Glaser. *Personal communication, Thesis in writing.* PhD thesis, TU Wien, Wien, 2015.

[HKW04] André Hedler, Siegfried Ludwig Klaumünzer, and Werner Wesch. Amorphous silicon exhibits a glass transition. *Nature Materials*, 3(11):804–809, November 2004.

[HKW05] A. Hedler, S. Klaumünzer, and W. Wesch. Boundary effects on the plastic flow of amorphous layers during high-energy heavy-ion irradiation. *Physical Review B*, 72(5):054108, August 2005.

[JHMR15] Andreas Johannes, Henry Holland-Moritz, and Carsten Ronning. Ion beam irradiation of nanostructures: sputtering, dopant incorporation, and dynamic annealing. *Semiconductor Science and Technology*, 30(3):033001, March 2015.

[JNP+14] A. Johannes, S. Noack, W. Paschoal, S. Kumar, D. Jacobsson, H. Pettersson, L. Samuelson, K. A. Dick, G. Martinez-Criado, M. Burghammer, and C. Ronning. Enhanced sputtering and incorporation of Mn in implanted GaAs and ZnO nanowires. *Journal of Physics D-Applied Physics*, 47(39):394003, October 2014. WOS:000341772000005.

[KPJ+13] Sandeep Kumar, Waldomiro Paschoal, Andreas Johannes, Daniel Jacobsson, Christian Borschel, Anna Pertsova, Chih-Han Wang, Maw-Kuen Wu, Carlo M. Canali, Carsten Ronning, Lars Samuelson, and Håkan Pettersson. Magnetic Polarons and Large Negative Magnetoresistance in GaAs Nanowires Implanted with Mn Ions. *Nano Letters*, 13(11):5079–5084, 2013.

[LW07] Charles M. Lieber and Zhong Lin Wang. Functional nanowires. *Mrs Bulletin*, 32(2):99–108, February 2007. WOS:000244600800011.

[Mö14] Wolfhard Möller. TRI3dyn – Collisional computer simulation of the dynamic evolution of 3-dimensional nanostructures under ion irradiation. *Nuclear Instruments and Methods in Physics Research Section B: Beam Interactions with Materials and Atoms*, 322:23–33, March 2014.

[MEB88] W. Möller, W. Eckstein, and J. P. Biersack. Tridyn-binary collision simulation of atomic collisions and dynamic composition changes in solids. *Computer Physics Communications*, 51(3):355–368, November 1988. 00441.

[MVB+06] J. Meijer, T. Vogel, B. Burchard, I. W. Rangelow, L. Bischoff, J. Wrachtrup, M. Domhan, F. Jelezko, W. Schnitzler, S. A. Schulz, K. Singer, and F. Schmidt-Kaler. Concept of deterministic single ion doping with sub-nm spatial resolution. *Applied Physics a-Materials Science & Processing*, 83(2):321–327, May 2006. WOS:000236641800028.

[Nas08] Nastasi/Mayer/Hirvonen. *Ion-Solid Interactions: Fundamentals and Applications*. Cambridge University Press, Cambridge ; New York, auflage: revised. edition, January 2008.

[NSUM14] Maureen L. Nietiadi, Luis Sandoval, Herbert M. Urbassek, and Wolfhard Möller. Sputtering of Si nanospheres. *Physical Review B*, 90(4):045417, July 2014.

[Ohd08] Iwao Ohdomari. Single-ion irradiation: physics, technology and applications. *Journal of Physics D: Applied Physics*, 41(4):043001, February 2008.

[PGL+14] Slawomir Prucnal, Markus Glaser, Alois Lugstein, Emmerich Bertagnolli, Michael Stoeger-Pollach, Shengqiang Zhou, Manfred Helm, Denis Reichel, Lars Rebohle, Marcin

Turek, Jerzy Zuk, and Wolfgang Skorupa. III-V semiconductor nanocrystal formation in silicon nanowires via liquid-phase epitaxy. *Nano Research*, 7(12):1769–1776, December 2014. WOS:000346641400006.

[PKB+12] Waldomiro Paschoal, Sandeep Kumar, Christian Borschel, Phillip Wu, Carlo M. Canali, Carsten Ronning, Lars Samuelson, and Hakan Pettersson. Hopping Conduction in Mn Ion-Implanted GaAs Nanowires. *Nano Letters*, 12(9):4838–4842, September 2012. WOS:000308576000069.

[PKJ+14] W. Paschoal, Sandeep Kumar, D. Jacobsson, A. Johannes, V. Jain, C. M. Canali, A. Pertsova, C. Ronning, K. A. Dick, L. Samuelson, and H. Pettersson. Magnetoresistance in Mn ion-implanted GaAs:Zn nanowires. *Applied Physics Letters*, 104(15):153112, April 2014. WOS:000335145200060.

[PMB04] Lourdes Pelaz, Luis A. Marqués, and Juan Barbolla. Ion-beam-induced amorphization and recrystallization in silicon. *Journal of Applied Physics*, 96(11):5947–5976, December 2004.

[rm15] ITRS road map. ITRS road map, April 2015.

[Sch12] Bernd Schmidt. *Ion beams in materials processing and analysis*. Springer, New York, 2012.

[SN06] Simon M. Sze and Kwok K. Ng. *Physics of Semiconductor Devices*. Wiley-Interscience, Hoboken, N.J, 3 edition edition, October 2006.

[SSK+11] Janusz Sadowski, Aloyzas Siusys, Andras Kovacs, Takeshi Kasama, Rafal E. Dunin-Borkowski, Tomasz Wojciechowski, Anna Reszka, and Bogdan Kowalski. GaAs–MnAs nanowires. *physica status solidi (b)*, 248(7):1576–1580, July 2011.

[TR95] H. Trinkaus and A. I. Ryazanov. Viscoelastic Model for the Plastic Flow of Amorphous Solids under Energetic Ion Bombardment. *Physical Review Letters*, 74(25):5072–5075, June 1995.

[Vol91] C. A. Volkert. Stress and plastic flow in silicon during amorphization by ion bombardment. *Journal of Applied Physics*, 70(7):3521–3527, October 1991.

[XYS+03] Y. Xia, P. Yang, Y. Sun, Y. Wu, B. Mayers, B. Gates, Y. Yin, F. Kim, and H. Yan. One-Dimensional Nanostructures: Synthesis, Characterization, and Applications. *Advanced Materials*, 15(5):353–389, March 2003.

[ZLB85] J. F. (James F.) Ziegler, U. Littmark, and J. P. Biersack. *The stopping and range of ions in solids / J.F. Ziegler, J.P. Biersack, U. Littmark*. The Stopping and ranges of ions in matter ; v. 1. Pergamon, New York, 1985. Includes index. Bibliography: p. 308-315.